https://doi.org/10.46813/2026-165-147

INFLUENCE OF THE COMPOSITION OF POLYMER-STEEL NANOMATERIALS ON RADIATION SHIELDING AND MECHANICAL CHARACTERISTICS

E.M. Prokhorenko[1], V.V. Lytvynenko[1,2], A.A. Zakharchenko[2], M.A. Khazhmuradov[2], S.A. Sokolov[2], T.G. Prokhorenko[3]

[1]Institute of Electrophysics and Radiation Technologies NAS of Ukraine, Kharkiv, Ukraine;
[2]NSC "Kharkiv Institute of Physics and Technology", Kharkiv, Ukraine;
[3]Kharkiv National Automobile and Highway University, Kharkiv, Ukraine
E-mail: prokhorenkoem@gmail.com

Work was completed to develop technological processes for the industrial production of radiation shielding composite material samples. The composites consisted of polystyrene, steel microparticles, and aluminum nanoparticles. The characteristics of radiation shielding composites with different component contents and particle sizes were examined. These composites can be used for both ionizing radiation shielding and electromagnetic radiation shielding. Composites in which the volumetric polystyrene content was slightly greater than the total metal content were studied. Ionizing radiation absorption coefficients were measured experimentally using standard gamma-ray sources (^{241}Am, ^{152}Eu). Ionizing radiation flux attenuation coefficients were determined using mathematical modeling methods (Monte Carlo method, Geant4 v11.04 code). The experimental results and calculated data show good agreement. Tensile strength tests on a break were conducted on composite material samples at temperatures of 250, 290, 320 K.

PACS: 81.05.Qk, 87.55K-, 87.55N, 61,80.Fe, 81.40.Wx

INTRODUCTION

Various types of ionizing radiation are widely used in the industrial and agricultural sectors, as well as in energy and medicine. The application of radiation technologies across diverse fields of human activity has significantly advanced these sectors.

Key properties of ionizing radiation include its ability to act at a distance and to penetrate deeply into the volume of the object under study. These characteristics enable the use of ionizing radiation for examining the internal structure of objects and for flaw detection.

Ionizing radiation is widely used in medicine for diagnostics, therapy, and the sterilization of medical equipment, instruments, and pharmaceutical products.

In agriculture, ionizing radiation is employed in a vast array of technological processes, such as stimulating crop growth, decontamination, and more.

The use of ionizing radiation in science also deserves special mention. A great number of ionizing radiation sources of various types are in operation at nuclear energy facilities.

Facilities involved in the extraction of radioactive isotopes play a significant role; waste rock storage sites and open-pit mines are particularly important in this context. Natural deposits of radioactive isotopes, granite formations, and similar geological features serve as sources of ionizing radiation.

Areas designated for the storage and disposal of spent nuclear fuel (SNF) and radioactive waste (RAW) – as well as equipment that has reached the end of its service life or failed – occupy a position of particular concern.

Consequently, the cumulative exposure of biological organisms (humans) to ionizing radiation is steadily increasing. Furthermore, the potential for critical incidents and accidents must be taken into account, as these events could lead to the release of ionizing radiation sources into the environment.

Exposure to ionizing radiation contributes to the onset and development of various diseases. Furthermore, ionizing radiation disrupts the stable operation of various types of equipment.

Protection against ionizing radiation is achieved through three primary methods: a) using low radiation doses and intensities, b) minimizing the time spent in the active zone, and c) creating a layer of radiation-shielding material.

The use of various radiation-shielding materials is an effective method of protection.

To protect against neutron fluxes, elements with low atomic mass and a wide cross-section are used (B, Br, various paraffins).

Traditionally, concrete structures with the addition of lead and oxides of heavy materials are used to protect against ionizing radiation. The technology for their production has been developed. They have high radiation protective characteristics.

These materials absorb X-ray and gamma radiation well, accelerated beams of high-energy protons, ions, and electrons. The main disadvantages of these protective materials are their significant weight, bulkiness, rigidity, and toxicity (presence of lead).

Therefore, the challenge lies in creating lightweight, versatile, and wear-resistant materials. Various composite materials are being developed for this purpose, specifically those based on polystyrene with various additives. These materials offer high strength and low density, while also being wear-resistant and flexible. Importantly, these polymer composites are lead-free.

Radiation-shielding composite materials were produced by blending a polymer matrix with radiation-shielding particles. High-atomic-number elements – such as tungsten, bismuth, or steel powders, mixtures of other

heavy materials, and heavy metal oxides – can be used as these shielding particles [1–9].

Work has been carried out to improve the production technology for radiation-shielding composite materials. The processes for mixing the composite components were refined, and the parameters for heating, curing, and polymerizing the mixture were established. It is also necessary to determine the shape and component composition of the composite material.

Pilot-scale batches of polystyrene-based composite materials were produced. Tungsten and steel powders were used as radiation-shielding additives, while aluminum powder was employed to form the composite matrix.

Composite materials of this type are used not only for radiation shielding but also for electromagnetic shielding.

The shielding mechanism varies depending on the content of the metallic component. At low metallic content, metal particles act as scattering centers, leading to the re-radiation of the incident wave. At high metallic content, the composite provides shielding by acting as a conductor.

PURPOSE OF WORK

The aim of this work is:

1. To refine the compression molding technology for composites based on a polystyrene matrix with a steel radiation-shielding additive. To determine processing parameters and composite compositions that enhance uniformity and strength. To select component materials and dimensions to improve interfacial compatibility between the matrix material and the functional radiation-shielding particles.

2. Experimental measurement of the change in gamma-ray exposure dose when using polystyrene-steel composite materials. Numerical calculation of gamma-ray absorption coefficients for composite layers of varying thickness.

3. Experimental measurement of tensile strength values for polystyrene-steel composite samples.

CONDUCTING EXPERIMENTS AND DISCUSSION OF RESULTS

PSM-115 (GOST 20282-86, TU U 24.4-00481318-025-2003) was used as the base material for the composite. Polystyrene is lightweight, exhibits high wear resistance, and is highly resistant to aggressive environments. It is easy to process, and a vast number of certified manufacturing procedures already exist for it. Polystyrene is well-suited for processing and the fabrication of various products. Given its softening temperature of 86…92 °C, and melting point of 198 °C, it is suitable for use under diverse climatic conditions and across a wide temperature range.

Note that polystyrene has a very important property. When polystyrene is irradiated with ionizing radiation, two opposite processes occur. One process is the process of destruction. The second process is the process of radiation crosslinking of polystyrene molecules [11].

The stitching process occurs as follows. As a result of exposure to ionizing radiation, polystyrene molecules are destroyed. But at the same time, open radicals are formed, which have the ability to interact with each other. As a result of the interaction of molecules, transverse covalent bonds are created between macromolecules. A spatial grid is formed. These processes slow down the destruction of polystyrene and improve its performance characteristics.

To provide radiation shielding, a component with a high atomic number is added to the composite. Materials such as tungsten, bismuth, lead, and steel are commonly used in practice. In this study, steel serves as the radiation-shielding component. The steel was utilized in the form of microparticles, with various particle sizes being employed. The choice of steel was based on its effective radiation-shielding properties. Another significant factor influencing the selection of the radiation-shielding component was the cost of the steel powder. The steel powder of the specified sizes was obtained from turning and grinding waste [12–14]. To produce particles of this size, the metal scrap (metal chips) underwent preliminary comminution and sorting.

Steel exhibits poor interfacial compatibility with polystyrene; steel particles are only weakly anchored within the polystyrene. To reinforce the composite, the polystyrene matrix was doped with nanoparticles characterized by a high coefficient of interfacial compatibility (wettability). Doping polymer matrices with nanoparticles enhances their properties, leading to increased bonding between polymer radicals and chains. Enhanced interaction between the filler nanoparticles and the polymer matrix results in greater composite strength and hardness. It is essential to use nanoparticles with a high surface-area-to-volume ratio; these particles disperse within the base matrix, forming an interfacial region and strengthening the bond between the particle surface and the matrix [11].

Aluminum powders were used to reinforce the composite material. The powders were derived from aluminum grades ASD-6, 2014, and 6111 (ISO 209-1, TU 1791-007-49421776-2011) [15, 16]. In accordance with standard specifications, the aluminum particles had sizes of 10…20, 30…40, and 70…80 μm. Aluminum exhibits high interfacial compatibility with polystyrene. Incorporating aluminum particles into the polystyrene matrix reinforces the material, thereby increasing its strength. The aluminum particles surround the steel microparticles, securing them within the composite; this leads to a significant increase in the composite material's strength.

Equipment improvement. Composite materials are produced using various methods [17]. In this study, several injection molding machines were employed. The majority of the work was carried out using a Windsor SP 80 horizontal injection molding machine (injection pressure: 180 MPa; injection volume: 50 cm^3). Originally, the Windsor SP 80 was a standard injection molding machine designed for the production of simple polystyrene products. The layout and design features of the Windsor SP 80 allowed for significant modernization and the implementation of upgrades to enable the production of polystyrene-steel composite materials.

The primary improvement was the addition of a second screw (plunger). This enables the separate feeding of the component mixture and polystyrene into the

extruder, thereby enhancing the uniformity of component distribution throughout the composite's volume. A second key modification involved installing a rotating device within the hopper, where the metal components are mixed. The hopper's rotation speed was adjustable, ranging from 4 to 70 rpm. This speed range allows for the selection of optimal operating conditions to achieve a more uniform composite structure.

The cooling process for the finished products was smoothly regulated. Additional heating elements were incorporated into the feedstock supply circuit. A temperature monitoring system for the equipment and feedstock was also implemented. Temperature monitoring was performed continuously, utilizing optical methods and infrared radiometry (using Lend Ti-814, Fluke-10, and Fluke-25 instruments).

Samples of polystyrene steel composites were fabricated. Composite materials of the PS08FeYYAlZZ type were obtained. The YY and ZZ values correspond to the number of steel and aluminum components. In accordance with the technological process, the content of components was measured in volumetric units. Therefore, the numbering of composites is given taking into account the number of volumetric parts of the components [7, 9]. Composites of the PS8Fe4Al3 type were manufactured. This composite material contained 8 volumes of polystyrene, 4 volumes of steel powder, 3 volumes of aluminum powder. The mass content of the components was as follows: PS – 0.182, Fe – 0.6504, Al – 0.1676. The density was 3.22 g/cm^3.

The steel particles had dimensions close to 280 μm. Steel chips obtained from lathe machining waste were used to produce the particles. The steel chips underwent preliminary comminution, followed by a sorting process using sets of sieves [12–14]. The aluminum powder consisted of particles with a standard size of 30…40 μm. During composite fabrication, the hopper rotation began at 20 rpm. Since aluminum and steel particles differ in size and weight, uniform mixing is achievable only at a specific rotation speed. An optimal rotation speed was determined for the steel powder and aluminum powder of these dimensions. Experimental testing established that the optimal hopper rotation speed is 42 rpm. At this speed, a uniform distribution of the steel and aluminum components within the mixture is observed.

Decreasing or increasing the rotation speed leads to mixture separation, resulting in component non-uniformity within the composite.

The composites were examined using a microscope, with analysis focused on the cross-section. It was found that the steel particles were uniformly distributed throughout the composite volume. All microparticles were surrounded by aluminum nanoparticles and embedded in the polymer matrix.

Samples of several types were produced. The composites were manufactured in the form of spheres, plates, and rods. Production focused primarily on composites in the form of spheres. The spheres varied in size. Composites with different component proportions had been investigated previously. Composites in which the volume of polystyrene significantly exceeded the volume of the metallic component were considered; these exhibited poor radiation-shielding properties and lower strength characteristics.

Measuring the absorbed dose. Experimental measurements of the absorbed dose were conducted for specific types of composite materials.

Samples measuring 7×4×1 cm were used for the measurements. Samples of these dimensions were suitable for mounting in the measurement equipment. Furthermore, such samples are convenient to install when constructing stationary shielding structures or protective screens.

Measurements were performed using an ^{241}Am ionizing radiation source with a gamma-ray energy of 60 keV [18–20]. The experiments were conducted using a setup designed and manufactured at the NSC “KIPT” [18]. An “Amptek” spectrometric system [19] was employed for the measurements; it consisted of a preamplifier, an “XR-100T” CdTe detector (dimensions 5×5×1 mm), and a “PX5” microprocessor-based signal processing unit [20]. Spectra were acquired over a period of 20 min, ensuring high statistical reliability of the results. The spectral line distribution was obtained [9, 21]. Based on these spectra, absorption coefficients in composite materials can be determined. Absorption coefficients were measured within specific energy range

Measurements were performed in the 13…20 keV range, as well as at 26.34 and 59.54 keV. The detector resolution was found to be 1.1% for the 59.54 keV peak and 3.3% for the 13.9 keV peak. To experimentally determine the absorbed dose coefficients, the variation in photopeak area at different energies was investigated. The photopeak area decreases as the absorbing properties increase.

Absorbed dose coefficients were determined for gamma quanta with an energy of 59.54 keV. The relative absorption coefficient ξ_{60} was determined from the expression:

$$\xi_{60} = 1 - \frac{S_i}{S_0},$$

where S_i – represents the photopeak areas measured in the presence of the shielding material, and S_0 – represents the photopeak area in the absence of the shielding material.

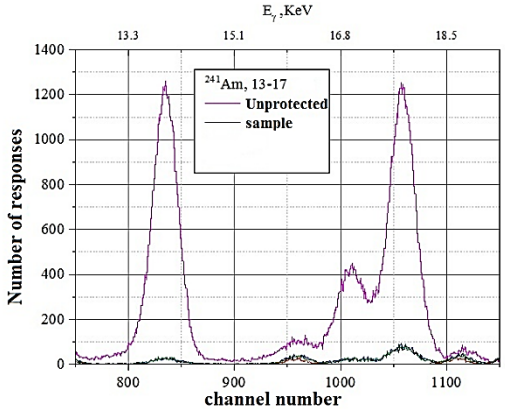


Fig. 1. Dynamics of the ^{241}Am photopeaks in the 13…18 keV range. With shielding material (blue line). Without shielding material (pink line)

To accurately determine the absorption coefficients, the following quantities were also calculated: the relative

absorption coefficient (ξ_γ), the linear absorption coefficient (μ_γ), the mass absorption coefficient (μ_γ/ρ) , and the tenth-value layer thickness for gamma-ray flux attenuation (L_{10}). The results are presented in [9, 21].

Absorption coefficients for gamma-ray photons with energies of 12…19 keV were also measured (Fig. 1).

From Fig. 1 shows that a significant number of gamma quanta with energies of 13…18 keV are absorbed. For gamma quanta with energies of 13.9 and 17.8 keV, the coefficients (ξ_γ, μ_γ, μ_γ/ρ , L_{10}) are given in Table 1.

Table 1

Coefficients ξ_γ, μ_γ, μ_γ/ρ , L_{10}, for gamma-ray quanta with energies of 13.9 and 17.8 keV

E_γ, keV	ξ_γ	μ_γ, 1/cm	μ_{14}/ρ, cm^2/g	L_{10}, cm
13.9	0.977	1.290	1.112	1.8
17.8	0.922	1.225	1.056	1.9

The key radiation-shielding characteristics of the composite materials are determined based on these parameters.

Absorption coefficients were measured in the energy range from 10 to 60 keV using an ^{241}Am ionizing radiation source.

For higher gamma-ray energies, absorbed dose measurements were performed using a ^{152}Eu gamma-ray quanta source [7, 9, 21]. The resolution for the 121.78 keV peak is 1.5%. Consequently, the ionizing radiation absorption coefficients of our composite materials can be experimentally determined over a wide range of gamma quanta energies. Notably, the majority of instruments used in medical diagnostics and materials science operate within the 10…120 keV energy range.

The radiation-shielding composite material is designed to reduce the exposure (absorbed) dose of gamma radiation. This radiation is generated by either medical diagnostic equipment or industrial fluoroscopic systems. The maximum gamma quanta energy in such systems does not exceed 150 keV; therefore, the absorption of gamma quanta with energies in this range was investigated.

Experimental measurements [7, 9, 21] indicate that a 10 mm thick PS8Fe4Al3 composite material completely absorbs gamma quanta with energies between 10 and 20 keV. Significant attenuation of the gamma-quantum flux also occurs in the 50 to 80 keV energy range. Effective protection against gamma quanta with energies exceeding 100 keV requires a substantial increase in the thickness of the PS8Fe4Al3 composite shielding layer.

Previous studies [3, 5, 7, 9, 21] investigated specific types of composite materials with varying component proportions or particle sizes.

Theoretical calculations of absorbed dose values were performed. The results of experimental measurements were found to be in close agreement with the theoretical calculations.

Calculation of radiation-shielding characteristics. Numerical modeling of the radiation-shielding properties of composite materials was performed using the Monte Carlo (MC) method. The Geant4 v11-04 software package [22] was employed. The model shown in Fig. 2 was used to calculate the ionizing radiation absorption coefficients of the composite material.

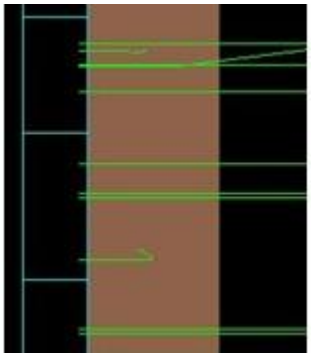


Fig. 2. Flow geometry model for calculating the absorption coefficient in a composite material (Geant4 method)

In the case of Geant4, we use a parallel beam of monoenergetic gamma quanta incident on a shielding layer of a specific thickness. We record the number of incident quanta at the surface and the number of absorbed quanta. At the exit from the layer, we record the spectrum of the emerging quanta.

In practical medical radiology, the XMuDAT software package [23, 24] is used to determine the mass absorption coefficient.

Absorbed dose calculations were performed for the composite material PS8Fe4Al3. One result was obtained using the Geant4 v11-04 software package, and the other using the XMuDAT software package. The results of the numerical calculations are presented in Fig. 3.

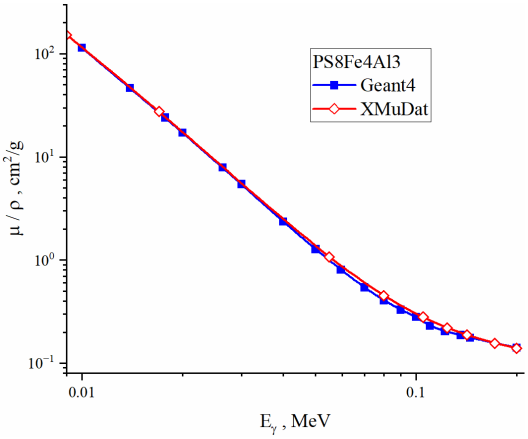


Fig. 3. Mass absorption coefficient of the polystyrene-steel composite PS8Fe4Al3

As shown in the graphs in Fig. 3, the calculation results are in good agreement. The results also show good agreement with experimental data [7, 9, 21]. Therefore, the Geant4 v11-04 software package was used for the calculations.

Table 2

Exposure dose in the absence of a protective layer. Gamma-quanta with energies of 60 keV

E_γ, keV	D_{air}, μR/quantum	±δ, %
60	$2.223 \cdot 10^{-5}$	2.17

D_{air} – calculated exposure dose in a modeled air volume.
δ – standard deviation (SD) of the exposure dose value.

The exposure dose in the absence of a protective layer was calculated using the Monte Carlo method. Gamma quanta with energies of 60 keV were used (Table 2).

For practical applications, the exposure dose in the presence of a protective layer is required. The dependence of the exposure dose on the thickness of the protective layer must be determined. Calculations of the exposure dose were performed for cases of attenuation by a factor of *e* (Table 3,a), two (Table 3,b), and ten (Table 3,c).

Table 3

Efficiency of exposure dose reduction for 60 keV gamma-rays near the exit surface of a polymer composite shielding sphere

a

Radiation dose	$H_{1/e}$, cm	$D_{1/e}$, uR/q	δ, %	$D_{air}/ D_{1/e}$
$D_{1/e}$	0.36	6.732E-05	2.38	0.330

b

Radiation dose	H_2, cm	D_2, uR/q	δ, %	D_{air}/ D_2
D_2	1.29	1.102E-05	4.24	2.017

c

Radiation dose	H_{10}, cm	D_{10}, uR/q	δ, %	D_{air}/ D_{10}
D_{10}	2.48	2.318E-06	7.02	9.594

$D_{1/e}$ – radiation dose. The thickness of the protective layer reduces the gamma-ray flux by a factor of **e**; D_2 – radiation dose. The thickness of the protective layer reduces the gamma-ray flux by a factor of two; D_{10} is the radiation dose. The thickness of the protective layer ensures a tenfold reduction in the gamma-ray flux; H_i – thickness of the protective layer for the options listed above; δ – standard deviation (SD) of the exposure dose value; D_{air}/D_i – the ratio of the radiation dose without a protective layer to that with a protective layer of thickness **i**.

For these thicknesses, gamma-ray spectra were obtained using numerical methods after the radiation had passed through the shielding layer. The incident gamma-ray energy was 60 keV.

Fig. 4 shows the gamma-ray spectra after passage through a shielding layer that attenuates the incident gamma-ray flux by a factor of *e*.

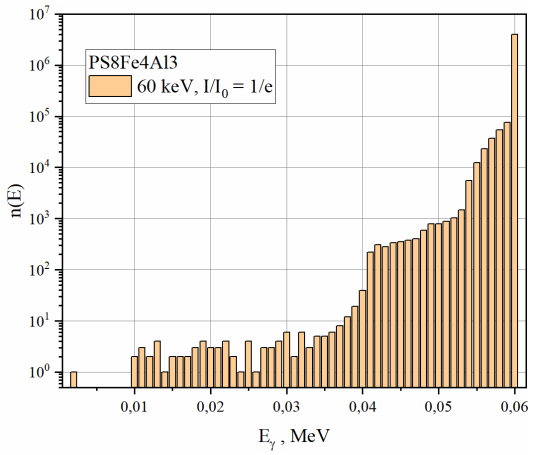


*Fig. 4. Gamma-ray quanta spectrum for attenuation by a factor of **e**. Initial energy: 60 keV. Shielding layer: PS8Fe4Al3 composite. Shielding layer thickness ($H_{1/e}$) was $1/\mu = 0.36$ cm*

Fig. 5 shows the spectrum for the case where the incident flux of gamma-ray quanta is attenuated by a factor of two.

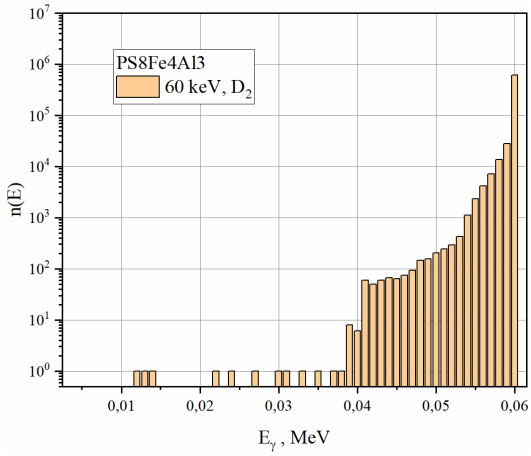


Fig. 5. Gamma-ray quanta spectrum for a twofold attenuation. Initial energy: 60 keV. Shielding layer: PS8Fe4Al3 composite. Shielding layer thickness (H_2): 1.29 cm

Fig. 6 shows the spectrum for the case where the incident flux of gamma-ray quanta is attenuated by a factor of ten.

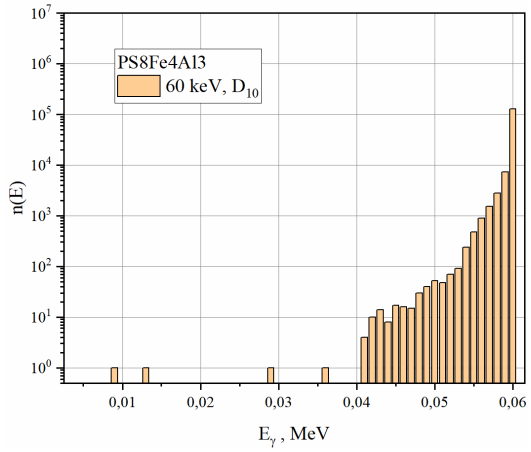


Fig. 6. Gamma-ray quanta spectrum for a tenfold attenuation. Initial energy: 60 keV. Shielding layer: PS8Fe4Al3 composite. Shielding layer thickness (H_2): 2.48 cm

For gamma-ray quanta with an initial energy of 60 keV and a shielding layer thickness of $1/\mu = 3.59$ mm, maximum absorption occurs in the range below 10 keV, with high absorption observed in the 10…38 keV range. The graphs show that as the number of gamma-ray quanta decreases by a factor of e ≈2.71828, a significant number of low-energy quanta appear; these quanta are the result of Compton scattering. Lower-energy gamma-ray quanta are absorbed more effectively by biological tissues. Consequently, near the exit surface of the shielding layer, the actual reduction in exposure (or absorbed) dose is significantly less than the reduction in the incident gamma-ray quanta flux.

To achieve a genuine reduction in radiation dose, an additional protective layer should be applied beyond the sphere with a thickness of $H_{1/e}$. This increases the total shielding thickness. Figs. 5 and 6 demonstrate that

increasing the shielding layer ensures the absorption of Compton (low-energy) gamma quanta; only isolated Compton gamma quanta originating in the near-surface layer are observed. A reduction in the number of gamma quanta in the 40…60 keV energy range is also evident. The thickness increased non-linearly as shielding performance was enhanced: the ratio $H_2/H_{1/e}$ is approximately 3.2–3.8, while the ratio $H_{10}/H_{1/e}$ is approximately 6.5–6.9.

These calculations are valid for a parallel beam of gamma quanta; under these conditions, the radiation dose is at its maximum. This factor must be taken into account when solving the inverse problem in medical radiology. In medical radiology, the delivery of the exact prescribed dose is essential during radiation therapy, as an inaccurate dose reduces treatment effectiveness.

It should be noted that if the radiation source is a point source or if gamma quanta are emitted over a significant solid angle, the absorbed dose depends on the square of the distance between the protective layer and the radiation source. In such calculations, the D_2 and D_{10} values would be lower than those obtained in our study. Nevertheless, our calculations remain valid because they represent the scenario of maximum ionizing radiation absorption; in practical applications, therefore, shielding with the composite material layer would be even more effective.

Tensile strength measurement. Strength and wear resistance are key characteristics in the practical application of composite materials. These properties are related to tensile or compressive strength; in this study, tensile strength was investigated.

A tensile testing machine was used for the experiments. Measurements were conducted in accordance with the requirements of GOST 11262-80 (“Plastics: Tensile properties”), ASTM D638-14, and ASTM D3039/D3039M [25, 26]. Specially shaped specimens were fabricated for the experimental measurements; these took the form of rods 12 cm in length and 1 cm in diameter. The following values were determined: tensile strength, elongation at break, and yield strength. Measurements were performed at temperatures of 250, 290, 320 K. These specific temperature points were selected because they correspond to temperatures naturally occurring on the European continent.

The PS8Fe4Al3 composite contains nearly equal volumetric proportions of polystyrene and metallic components. This allows for maximum loading of the polystyrene matrix with aluminum nanoparticles and steel microparticles. Processing parameters were optimized to achieve a homogeneous distribution of the components throughout the composite material. Cross-sections of the composite samples were examined using a Bresser 2500 microscope, revealing a uniform distribution of metal particles within the composite. Notably, the steel microparticles were anchored within the polystyrene by the aluminum nanoparticles; the aluminum nanoparticles enveloped and surrounded the steel particles, thereby enhancing the composite's strength.

It was found that at a temperature of 290 K, the tensile strength was 42.8 MPa. At 320 K, the strength was 42.4 MPa. At 250 K, the tensile strength was 41.6 MPa.

The fracture surfaces were examined using a Bresser 2500 microscope. At temperatures of 290 and 320 K, the fracture exhibited an elongated shape, and necking was observed. In the case of the fracture at 320 K, the neck was more elongated and thinner. Elongated polystyrene segments were observed in the fracture zone; this resulted from the heating and softening of the polystyrene, allowing the long polymer molecules to slide parallel to one another. At 250 K, the strength was slightly lower, as the polystyrene underwent embrittlement. Fracture occurred via cleavage, with the cleavage plane running across the neck. The cleavage occurred primarily along the steel particles, and the fracture surface displayed a pattern of small, randomly distributed steps.

Thus, we have determined the trends in tensile strength variation across a wide temperature range, enabling us to predict how composite strength will change under various temperature and weather conditions.

Our findings align with research on composites of similar composition. For instance, studies [27, 28] report results on compressive strength measurements for polyethylene-zinc composites. The results presented in [27, 28] are generally consistent with those obtained in our own research; the agreement regarding the trends in strength variation is particularly notable.

Based on the obtained results, we can determine the attenuation of the incident ionizing radiation flux (specifically 60 keV gamma-ray photons) for various thicknesses of a polystyrene-steel composite shielding layer. For applications in medical radiology (radiation therapy), we can calculate the radiation dose absorbed by the irradiated object. Furthermore, based on measured strength data, we can determine the maximum dimensions of the shielding layer and the conditions under which it retains its mechanical properties.

CONCLUSIONS

1. The equipment for producing polystyrene-metal composite materials has been upgraded. An additional mixture component mixing system and a preheating system were added to the basic equipment setup. The composite homogeneity monitoring system was improved using optical and IR-radiometric instruments. Heating parameters and processing speeds were optimized for the manufacture of PS8Fe4Al3 composite materials, and the production process itself was refined. These improvements were implemented for composites utilizing steel powder microparticles (280 μm) and aluminum powder nanoparticles (30…40 μm).

2. Numerical methods were used to simulate the absorption of a flux of γ-quanta (initial energy 60 keV). Spectra of γ-quanta were obtained at the exit from protective layers of different thicknesses. The spectra were obtained for the PS8Fe4Al3 composite material. It was found that a PS8Fe4Al3 composite layer with a thickness of 3.59 mm weakens the flux of γ-quanta by a factor of e. A composite layer with a thickness of 1.29 cm weakens the flux of γ-quanta by 2 times. A composite

layer with a thickness of 2.48 cm weakens the flux of γ-quanta by 10 times.

3. Tensile strength limits were determined using a tensile testing machine. For the PS8Fe4Al3 composite material, tensile strength was measured at fixed temperatures of 250, 290, 320 K. The maximum tensile strength value was 42.8 MPa, obtained at 290 K. Fracture occurred with necking (at 290 K). Fracture morphologies were characterized: at 250 K, the fracture was of the cleavage type, whereas at 320 K, it involved drawing. The fracture process was accompanied by necking and the sliding of individual long molecules.

REFERENCES

1. Chenhao Zeng, Qing Kang, Zhongshan Duan, Bing Qin, Xiaojie Feng, Haoyuan Lu, Yuanye Lin. Development of Polimer Composites in Radiation Shielding Applications: A Reviev // *Jornal of Inorganic and Organometallic Polymers and Materials*. 2023, v. 33, p. 2191-2239.

2. A.H. Abdalsalam et al. Investigation of gamma ray attenuation features of bismuth oxide nano powder reinforced high-density polyethylene matrix composites // *Radiat. Phys. Chem.* 2020, v. 1(168), p. 108537.

3. E.M. Prokhorenko, V.V. Lytvynenko, A.A. Zaharchenko, M.A. Hazhmuratov, T.G. Prokhorenko. Studying the changes in the characteristics of radiation-protective composition materials in dependence on homogeneity of distributing of metal components // *Problems of Atomic Science and Technology*. 2019, № 2(120), p. 121-126;
https://doi.org/10.1016/j.net.2020.03.029

4. Chaitali V. More et al. Polymeric composite materials for radiation shielding: a review // *Environ Chem Lett*. 2021, № 19, p. 2057-2090;
https://doi.org/10.1007/s10311-021-01189-9

5. E.M. Prokhorenko, V.V. Lytvynenko, A.A. Zaharchenko, M.A. Hazhmuratov, T.G. Prokhorenko. Study of strength characteristics and radiation protective properties of polystyrene tungsten composite materials // *Problems of Atomic Science and Technology*. 2023, № 2(144), p. 29-36.

6. U.C. Okonkwo, C.I. Idumah, C.E. Okafor, C.C. Ohagwu, M.E. Aronu, I.P. Okokpujie, N.N. Chukwu, C.E. Chukwunyelu. Development, characterization, and properties of polymeric nanoarchitectures for radiation attenuation // *J. Inorg. Organomet. Polym. Mater*. 2022, v. 32, p. 4093-4113.

7. E.M. Prokhorenko, V.V. Lytvynenko, A.A. Zaharchenko, M.A. Hazhmuratov, S.A. Sokolov, T.G. Prokhorenko, A.P. Ben. Analysis of radiation protective properties of polystyrene – based composite materials // *Problems of Atomic Science and Technology*. 2021, № 3(133), p. 111-118;
https: //doi.org/10.46813/ 2021-133-111

8. J. Sangeetha, S. Thangavelu, P. John. A review on polymer nanocomposites as lead-free materials for diagnostic X-ray shielding: Recent advances, challenges and future perspectives // *Hybrid Edvanced*. 2023, v. 4, p. 100100; Doi 10.1016/j.hybadv.2023.100100

9. E.M. Prokhorenko, A.A. Zaharchenko, M.A. Hazhmuratov, S.A. Sokolov, T.G. Prokhorenko. Radiation shielding characteristics and characteristics of strength from polystyrene steel composite materials with high metal content // *Problems of Atomic Science and Technology*. 2025, № 3(157), p. 127-133;
https: //doi.org/10.46813/ 2025-157-127

10. Qian Li, Yaping Wang, et al. Research on X-ray shielding performance of wearable Bi/Ce-natural leather composite materials // *Journal of Hazardous Materials*. 2020**,** v. 398, p. 122943.

11. K. Sudheendra, J. Vinodhini, M.K. Pitchan, G.A. Mannadiar, S. Bhowmik. *Effect of High-Energy Radiations on High Temperature-Resistant Thermoplastic Polymeric Composite for Aviation, Space, and Nuclear Applications*. 2023, 15 May, p. 219-233.

12. E.M. Prokhorenko, V.V. Lytvynenko, O.A. Melyakova, Yu.F. Lonin, A.G. Ponomarev, V.T. Uvarov, N.A. Shul'gin, T.G. Prokhorenko, R.I. Starovoytov, A.I. Morozov, S.R. Artemev. Strengthening of the surface of steel (9KhFM) exposed to a high-current electron beam // *Problems of Atomic Science and Technology*. 2020, № 1(125), p. 167-172.

13. E.M. Prokhorenko, V.F. Klepikov, V.V. Lytvynenko, P.A. Khaymovich, N.A. Shul'gin, A.I. Morozov. Diagnostics of processes of wear of materials of balls drum mills // *Eastern European Journal of Enterprise Technologies*. 2015, №1/5, v. 73, p. 14-20.

14. E.M. Prokhorenko, V.V. Lytvynenko, O.A. Melyakova, Yu.F. Lonin, A.G. Ponomarev, V.T. Uvarov, N.A. Shul'gin, T.G. Prokhorenko. Modification of structure of the surface of steel (KhGS) as result of influences of high-current electron beem // *Problems of Atomic Science and Technology*. 2020, № 2(126), p. 47-53.

15. E.M. Prokhorenko, V.V. Lytvynenko, V.V. Bryukhovetskiy, N.A. Shul'gin, I.V. Kolodiy, I.G. Tantsyura, T.G. Prokhorenko. Modification of the structurally the phase state of aluminum alloy as a result of radiation thermal treatment // *Problems of Atomic Science and Technology*. 2022, № 1(137), p. 122-129;
https://doi.org/10.46813/2022-137-122

16. E.M. Prokhorenko, V.V. Lytvynenko, N.A. Shul'gin, I.V. Kolodiy, I.G. Tantsyura, T.G. Prokhorenko. Changes in the structure and phase state of aluminum alloy 2014, which occurred as a result of irradiation with an electron beam // *Problems of Atomic Science and Technology*. 2024, № 1(149), p. 82-89.

17. Seon-Chil Kim. Fabrication Process and Particle Dispersion Characteristics of W–PETG-Based 3D-Printed Composites for Medical Radiation Shielding // *Polymers*. 2026, № 18(2), p. 268;
https://doi.org/10.3390/polym18020268

18. V.E. Kutnij, A.V. Rybka, L.N. Davydov, A.A. Zakharchenko, D.V. Kutnij, A.S. Abyzov. *Detektory ioniziruyushih izluchenij na osnove tellurida kadmiyatsinka*. Kharkov: Tipografiya Madrid, 2021, 352 p. (in Ukraine).

19. https://www.amptek.com/internal-products/xr-100 cdte-x-ray-and-gamma-ray-detector.

20. A.A. Zakharchenko, V.E. Kutny, A.V. Rybka, et al. Application of gamma-spectrometer on the basis of CdTe in dosimetry of high-energy bremsstrahlung // *Problems of Atomic Science and Technology*. 2018, № 3(115), p. 123-127.

21. E.M. Prokhorenko, V.V. Lytvynenko, A.A. Zaharchenko, M.A. Hazhmuratov, S.A. Sokolov, T.G. Prokhorenko, A.P. Ben. Brief overview on research and development of radiation shielding protective composite materials based on polystyrene // *Problems of Atomic Science and Technology*. 2024, № 2(150), p. 107-114; https: //doi.org/ 10.46813/ 2024-150-107

22. J. Allison, K. Amako, J. Apostolakis, et al. Recent developments in Geant4 // *Nulc. Instrum. Meth. A*. 2016, v. 835, p. 186-225; https://doi.org/10.1016/j.nima.2016.06.125 1,2

23. XMuDat: Photon attenuation data on PC. Version 1.0.1 of August 1998. Summary documentation// https://inis.iaea.org/records/eaytw-1cn96

24. Comparison of x-ray cross sections for diagnostic and therapeutic medical physics // *Med. Phys*. 1996 Dec., v. 23(12), p. 1997-2005; https://doi.org/10.1118/1.597899

25. ASTM D638-14. Standard test method for tensile properties of plastics // *ASTM International, West Conshohocken, PA, USA*. 2014, p. 16.

26. ISO 527-1:2019 "Tensile tests on plastics" 7 p.; https://standards.iteh.ai/catalog/standards/sist/926d5ea4-e0ad-4a58-b318-. 520f53bb3c85/iso-527-1-2019

27. Farzad Isazadeh, Akbar Abdi Saray. Experimental and simulation assessment of gamma-radiation shielding properties of the polyester polymer reinforced with WO_3 // *Scientific Reports*. 2025, v. 15, p. 37145.

28. N. J. Abualroos, M.I. Idris, H. Ibrahim, M.I. Kamaruzaman, R. Zainon. Physical, mechanical, and microstructural characterisation of tungsten carbide-based polymeric composites for radiation shielding application // *Scientific Reports*. 2024, v. 14, p. 1375.

Article received 14.09.2026

ВПЛИВ СКЛАДУ ПОЛІМЕРНО-СТАЛЕВИХ НАНОМАТЕРІАЛІВ НА РАДІАЦІЙНО-ЗАХИСНІ ТА МЕХАНІЧНІ ХАРАКТЕРИСТИКИ

Є.М. Прохоренко, В.В. Литвиненко, О.О. Захарченко, М.А. Хажмурадов, С.О. Соколов, Т.Г. Прохоренко

Виконано роботи з розробки технологічних процесів промислового виготовлення зразків радіаційно-захисних композиційних матеріалів. Композити складалися з полістиролу, мікрочастинок сталі та наночастинок алюмінію. Розглядалися характеристики радіаційно-захисних композитів, які мали різний вміст компонентів та різні розміри частинок компонентів. Ці композити можуть використовуватися як захист від іонізуючого випромінювання, так і захист від електромагнітного випромінювання. Вивчалися композити, у яких об'ємна кількість полістиролу трохи більше сумарного об'єму металевої компоненти. Експериментальним шляхом було виміряно коефіцієнти поглинання іонізуючого випромінювання. Вимірювання виконували за допомогою еталонних джерел гамма-випромінювання (^{241}Am, ^{152}Eu). Коефіцієнти ослаблення потоку іонізуючого випромінювання знайдено за допомогою методів математичного моделювання (метод Монте-Карло (МС), код Geant4 v11.04). Результати експериментальних вимірювань та розрахункові дані мають гарний збіг. Для зразків композиційного матеріалу за температур 250, 290, 320 К проведено експерименти з знаходження межі міцності на розрив.